



# Printing and dyeing of halloysite nano clay hybrid with natural chlorophyll dye on cotton fabric

Daniel López-Rodríguez<sup>a,\*</sup>, Jorge Jordan-Nuñez<sup>b</sup>, Bàrbara Micó-Vicent<sup>b</sup>, Antonio Belda<sup>c</sup>

<sup>a</sup> Departamento de Ingeniería Textil y Papelera, Universitat Politècnica de València, Plaza Ferrándiz y Carbonell s/n, Alcoi, Spain

<sup>b</sup> Departamento de Ingeniería Gráfica, Universitat Politècnica de València Plaza Ferrándiz y Carbonell s/n, Alcoi, Spain

<sup>c</sup> Departamento de Ciencias de la Tierra y del Medio Ambiente, Universidad de Alicante, Ctra, San Vicente s/n, San Vicente del Raspeig, Spain

## ARTICLE INFO

### Keywords:

Halloysite  
Chlorophyll dye  
Dye adsorption  
Clay pigment  
Natural dye  
Printing natural dye  
Hybrid pigments  
TGA  
FTIR  
XRD

## ABSTRACT

This work deals with the synthesis of hybrids formed by the natural dye chlorophyll and halloysite for their subsequent application in the textile field. Once the pigments have been synthesized, with 98 % adsorption, they are used for two textile colouring functions, namely printing and dyeing. In both cases, satisfactory and interesting results were obtained. The hybrids were characterized by FTIR, XRD, TGA, SEM-EDX, BET and all the appropriate colour measurements were carried out to obtain the coordinates in CIELAB space and also to know their total solar reflectance (TSR) 45.98 %. In addition, statistical techniques were used with the use of ANOVA to evaluate the results obtained. The dyeing was carried out by exhaustion and its use was compared with the use of nibbled and non-nibbled fabrics. The textiles were tested for fastness and the results are presented in instrumentally obtained grey scale values, achieving in some cases values of 4–5. Thus, the chlorophyll adsorption capacity of halloysite and its stabilisation for subsequent application in printing and dyeing processes on textile substrates has been demonstrated. This process could be scalable at an industrial level.

## 1. Introduction

The concept of a circular and sustainable economy is becoming a hugely significant criteria in the realms of product and process design. Presently, many industries and researchers are actively engaged in crafting eco-friendly products and advancing sustainable practices, with natural dyes being a prominent example of this trend [1]. In South America, the production of these dyes is experiencing remarkable growth as dyes are successfully extracted from agricultural waste [2–5]. Natural dye derived from these dyes have several advantages. In addition to being non-toxic, they possess antioxidant properties, are suitable for medical applications and have the ability to biodegrade without causing environmental problems [4–8]. Among the most abundant and biologically significant natural pigments is chlorophyll, which is present in both eubacteria and plants [9].

Today, the textile industry is looking for sustainable and environmentally friendly alternatives, and natural dyes are becoming more and more prominent. These pigments extracted from plants, fruits and minerals offer an eco-friendly option compared to conventional chemical dyes [10,11]. Their use not only reduces the environmental footprint, but also benefits the health of workers and consumers by

minimising exposure to toxic substances. In addition, natural dyes provide unique and varied shades, inspired by the diversity of nature. This focus on sustainability in the choice of dyes reflects a growing commitment by the textile industry to more responsible and conscientious practices [12–14].

Chlorophyll dyes (CDs) have found applications in various fields due to the inherent properties of chlorophyll. These dyes have been used in biomedical applications [15], as well as in more complex applications, such as in the colouring of solar cells [16,17] and in the creation of supramolecular structures [18]. However, it is important to note that CDs show some instability when subjected to oxygen-rich atmosphere, elevated temperatures or high ambient light, which affects their antioxidant capacity [16,17].

Halloysite (HA), a versatile clay mineral, has emerged as an innovative solution in the textile industry for dye trapping. Its porous structure allows efficient absorption of pigments, effectively trapping them during dyeing processes [19]. This approach offers significant environmental benefits by reducing the release of toxic dyes into industrial wastewater. Halloysite not only acts as an effective fixing agent but is also a sustainable alternative that contributes to eco-efficiency in textile production. By adopting this technology, the industry is moving

\* Corresponding author.

E-mail address: [dalorod@upv.es](mailto:dalorod@upv.es) (D. López-Rodríguez).

<https://doi.org/10.1016/j.dyepig.2024.112352>

Received 4 April 2024; Received in revised form 18 July 2024; Accepted 22 July 2024

Available online 23 July 2024

0143-7208/© 2024 The Authors. Published by Elsevier Ltd. This is an open access article under the CC BY license (<http://creativecommons.org/licenses/by/4.0/>).

towards more responsible practices, demonstrating that innovation and sustainability can go hand in hand in the quest for cleaner textile solutions [20,21].

Mordants play a crucial role in the process of dyeing textiles with natural dyes, improving the adhesion and durability of the colour. These substances, which may be metallic salts such as alum or organic compounds such as tannin, act as fixing agents by forming bonds between the dyes and the textile fibres. By applying a mordant before dyeing, the surface of the fibre is prepared to receive the colour in a more uniform and permanent way [22,23]. Besides, the metal ions present in mordants can interact with the functional groups of dyes and fibres, creating chemical bonds that ensure a stronger colour fastness [24–26].

In addition to improving colour adhesion, mordants can also alter the shade and intensity of natural dyes, allowing for a greater variety of shades in dyed textiles. However, it is important to use mordants with caution, as excessive use can affect the softness and texture of fabrics, as well as pose environmental risks if residues are not properly managed.

It should be noted that this work compares the effect of performing different types of textile dyeing using the combination of the natural dye chlorophyll, mordants and nano clays. The combined effect of these three elements constitutes a totally novel and unprecedented technique. Thus, with the study of these variables we hope to obtain conclusive data on which are the best options to use and apply the hybrids of dye and clay, in order to scale them up to an industrial level in future works.

In addition, there are several benefits of dyeing or printing cotton fabrics with chlorophyll. Copper has inherent antimicrobial properties, which means that fabrics dyed with this dye can inhibit the growth of bacteria and other microorganisms [27–30]. This is especially beneficial for applications in garments, bedding, towels and other textiles that are in direct contact with the skin. Copper-based dyes tend to be more stable and resistant to fading by light and washing compared to other natural dyes [31–33]. This ensures longer colour durability in cotton fabrics.

Copper has antioxidant properties, which can help protect fabrics against oxidative deterioration, prolonging the life of the dyed material [34–37]. Cu-based chlorophyll dye can give fabrics increased UV resistance, protecting the cotton fibre and users from sun damage. Natural dyes, including those derived from chlorophyll, are generally more sustainable and environmentally friendly than synthetic dyes. Using Cu-based chlorophyll can reduce the environmental impact associated with the dyeing process.

Compared to some synthetic dyes, chlorophyll-based dyes are less toxic and safer for both textile workers and end consumers. Chlorophyll dyes can provide natural and pleasant green tones that are difficult to achieve with synthetic dyes. This is especially valued in sustainable fashion and products aiming for a natural and ecological look. Fabrics treated with copper-based dyes can offer additional health benefits due to copper's antimicrobial properties, making them suitable for medical and sportswear.

The process of dyeing cotton with natural and synthetic dyes has significant differences in terms of cost [38], environmental impact and sustainability. When comparing these two types of dyes, it is essential to consider several key aspects that affect both manufacturers and the environment [39].

Natural dyes are obtained from sources such as plants, insects and minerals. Common examples include indigo, turmeric and cochineal. These dyes are inherently more expensive due to the manual collection and intensive processes required for extraction and preparation. In addition, natural dyes require the use of mordants, such as alum and tannins, to fix the colour in the fabric, which adds an additional cost [40, 41]. The colour saturation obtained with natural dyes is usually lower, and often the process needs to be repeated for optimal results.

On the other hand, synthetic dyes are chemically synthesized products, mainly derived from petroleum and other compounds. Their mass

production and the automation of processes make them much more accessible and economical. The efficiency of these dyes is remarkably high; they provide intense and long-lasting colour saturation without the need for additional mordants, which further reduces production costs [42].

In terms of environmental impact, natural dyes have advantages and disadvantages. They are biodegradable and non-toxic, which means they do not pollute water and are safe for the environment. However, their production can require large areas of agricultural land and intensive use of water, which poses challenges in terms of sustainability on a large scale. Despite these drawbacks, natural dyes can be integrated into sustainable and renewable agricultural practices if properly managed.

Synthetic dyes, although economical and efficient, have a more negative environmental impact. The chemicals used in their manufacture are often toxic and can pollute water and generate hazardous waste [43]. In addition, the production of these dyes relies on non-renewable resources such as oil, which exacerbates their long-term sustainability profile.

In an overall analysis, natural dyes have a higher initial cost due to the collection and preparation required but are less polluting and safer for the environment. However, they can contribute to deforestation and intensive water use [44]. Synthetic dyes, although cheaper and more efficient in their application, are more polluting and rely on non-renewable resources, generating non-biodegradable waste that negatively impacts the environment.

## 2. Methodology

### 2.1. Materials

Today, researchers are actively exploring the application of nanotechnologies in adsorption processes, deeming it a highly efficient method for the removal of various highly detrimental pollutants from water. Clay minerals, in particular, have garnered significant attention due to their natural origin, synthesizability, and distinctive characteristics [45]. Halloysite, a 1:1-type clay mineral abundantly found in natural environments, has been hailed as an environmentally friendly material. Was purchased from the supplier Sigma-Aldrich (CAS number: 1332-58-7; CE number: 310-194-1). The nanotubes of halloysite (depicted in Fig. 1) have diameters ranging from approximately 40 to 70 nm and lengths spanning from 200 to 2000 nm [46]. The authors have determined their specific surface area (SSA) to be  $48 \text{ m}^2 \text{ g}^{-1}$  and cation exchange capacity (CEC) to be  $9.45 \text{ cmol kg}^{-1}$  [47]. These nanotubes often exhibit interstratified phases, with a CEC ranging from 31 to 73  $\text{cmol kg}^{-1}$  clay [48]. The external layer, predominantly composed of  $\text{SiO}_2$ , carries a negative charge, while the inner region, consisting of  $\text{Al}_2\text{O}_3$ , bears a positive charge [49]. The increased use of halloysite nanotubes (HNT) can be attributed to their cylindrical nature and specific properties, including a large surface area relative to their size, productivity, and stability at high temperatures [46,50–52].

To comprehend these distinctive properties, it's essential to recognize that HA belongs to the aluminosilicate family, characterized by alternating layers of octahedral aluminum oxide and tetrahedral silica. The incongruity between these two layer types results in the formation of a characteristic hollow tubular structure, giving rise to specific features derived from its nanoarchitecture [53]. It's noteworthy that the properties of HA are primarily influenced by the particular geological formation where they are found, as detailed in the available literature [53–58]. Due to their biocompatibility, halloysite have been extensively used to adsorb various dyes [59,60], including methylene blue (MB) [61–69], azo-dyes [70–76], triaryl and diaryl methane dyes [77–85], and xanthine dyes [59,86–88]. In a notable study, the combination of HA with zinc oxide nanoparticles and photocatalytic degradation

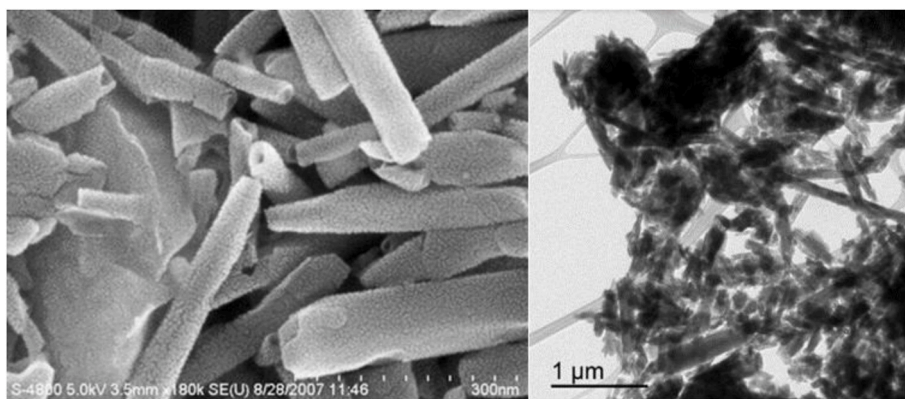


Fig. 1. Scanning electron microscope (SEM) images of the halloysite nano clay. TEM (right) and SEM (left).

succeeded in purifying up to 93 % of the Orange G dye both in waters obtained from real industrial discharges and from those carried out by laboratory simulation [89].

However, a common challenge with natural halloysite lies in its high concentration of impurities, to the removal of which is necessary to enhance adsorption capacity. Some researchers propose enhancing adsorption performance through a 12-h acid treatment and laminar surface injection [90]. Fig. 2 shows a simulation of what the HA structure looks like.

Copper chlorophyll with colour index 75810 and chemical formula ( $C_{34}H_{31}CuN_4Na_3O_6$ ), was purchased from the supplier Sensient® (Milwaukee, WI, USA) (CAS number: 11006-34-1; CE number: 234-242-5) (Fig. 3). This is a fascinating compound that offers a unique window into the world of biology and biochemistry and is an anionic dye in aqueous solution. Unlike ordinary chlorophyll, which contains magnesium in its core structure, copper chlorophyll has a copper atom in its nucleus. This variant of chlorophyll is found in microbial organisms called bacteriochlorophyll. These bacteria, which inhabit extreme environments such as saline lake sediments or anoxic environments, depend on sunlight for photosynthesis, but due to the scarcity of light in these habitats, they have evolved to use specific wavelengths of light that can penetrate these depths.

The presence of copper instead of magnesium in the chlorophyll molecule significantly alters its optical and electronic properties. This allows these bacteria to exploit near-infrared light, a region of the electromagnetic spectrum that contains lower energy than the visible light used by higher plants. By capturing this infrared light, the bacteria can photosynthesise even in limited light conditions, giving them an adaptive advantage in their unique and challenging habitats.

In addition to its importance in environmental biology, copper chlorophyll has also attracted interest in fields such as photovoltaic technology and bioenergy. Researchers are exploring ways to harness the unique properties of this molecule to develop new solar energy capture and conversion technologies, which could lead to significant advances in the efficiency of solar devices and the sustainable

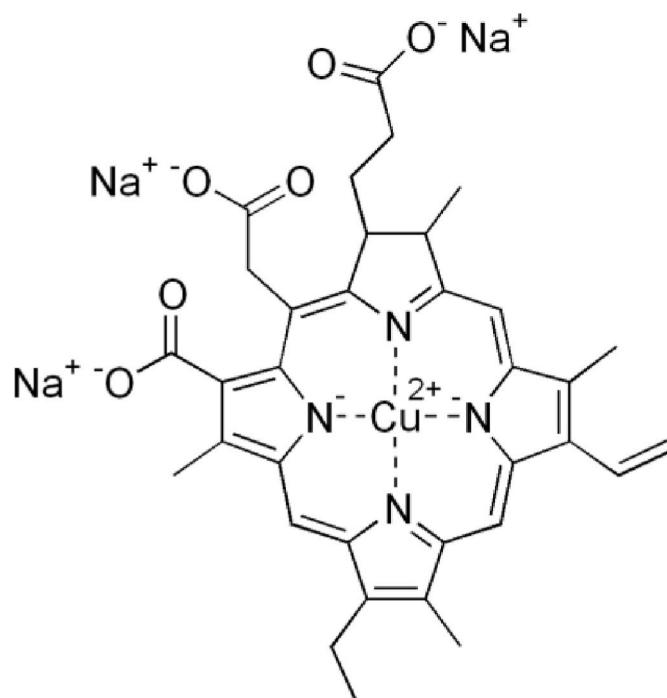


Fig. 3. Chemical structure of copper chlorophyll.

production of biofuels.

## 2.2. Methods

### 2.2.1. Adsorption methods

The process of adsorbing chlorophyll dye onto tubular nano-adsorbent was conducted using water as the solvent and by means of the stirring technique. In this research, nanotubular halloysite (HA) was dispersed at 1800 rpm for 20 h. The halloysite clay underwent heat treatment for 20 h at 210 °C and was then dispersed in deionised water at a concentration of 25 g L<sup>-1</sup>. To adjust the pH to -4, 37 % hydrochloric acid was used. The amount of dissolved dye was maintained at 2·10<sup>-3</sup> M.

Dye exchange was initiated by stirring at 2000 rpm for 4 h, followed by 500 rpm for 20 h. Separation of the solvent was achieved through centrifugation to obtain the paste-nano-pigment (PNP). Afterwards, the PNP underwent washing by dispersing its paste at 300 rpm for 40 min until the supernatant became clear. All separated supernatants from the initial step to the final washing were collected. The hybrid formed by the clay and the dye was gathered and dried for 2 h at 60 °C before being stored (Fig. 4).

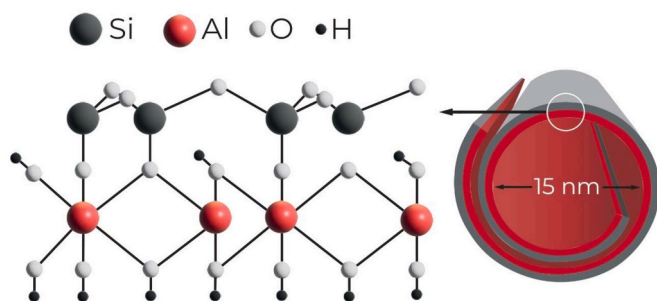


Fig. 2. Representation of the tubular structure of halloysite HA.



Fig. 4. HA + chlorophyll hybrid.

Before collecting the supernatants, measurements were carried out to avoid possible oxidation of the dye and alteration of the results. To complete the absolute adsorption of the dye which had not been trapped by the nano clay, both water and wash solution were kept shielded from light and temperature by storing them in airtight containers wrapped in aluminium foil. Afterwards, the separated supernatants were adjusted to a predetermined volume for subsequent spectrophotometer analyses.

### 2.2.2. Dyeing

The phenomenon of desorption refers to the process in which dye molecules move from the adsorbed phase, when they are trapped within a given solid, to a liquid phase [91,92]. Various research papers [93–95] outline different hypothesis regarding the isotherms governing this desorption, categorizing them as continuous desorption/adsorption systems that are not ideal and can be reversed. One model describes a scenario where the interaction among adjacent active sites is inconsistent due to the non-uniformity of the adsorbate, leading to non-homogeneous adsorption process. Each of these hypotheses contributes to our understanding of the real reason why the adsorption/desorption mechanism occurs.

Authors Momina, Shahadat Mohammad, and Suzylawati Isamil [96] present a desorption model for methylene blue (MB) involving subjecting the hybrid to elevated temperatures to weaken the bonds, followed by the use of a range of solvents such as HCl, ethanol, nitric acid, or acetone. They argue that any single phase alone is not adequate to achieve satisfactory desorption results.

This study introduces a simultaneous desorption-dyeing process, which builds on the concept that temperature weakens the bond between clay and dye [96], subsequently leveraging the inherent affinity

between dye and fibre using a conventional dyeing process. This approach facilitates the complete migration of dye from the halloysite to the textile fibre (refer to Fig. 5). Moreover, in the model proposed in this work, heat is applied through convection rather than radiation, unlike the model by Momina, Shahadat Mohammad, and Suzylawati Isamil, as convective heat proves more efficient in reaching broader areas of the clay and possesses higher energy levels.

The clay-dye hybrid is then used as a dyeing material for dyeing by exhaustion, using a bath ratio of 1/40. For the dyeing of a 100 % cotton (CO) a fabric with a grammage of  $135 \text{ g m}^{-2}$ ,  $25 \text{ yarns}\cdot\text{cm}^{-1}$ ,  $22 \text{ weft}\cdot\text{cm}^{-1}$  of plain weave. The yarn count in both warp and weft is 35 tex. The cotton fabric was mordanted to study the effect of these mordants in improving fastness and increasing the impact of the dye on the fibre by increasing its absorption. This mordanting is summarised in Table 1. The hybrid CPHA is used, 20 % o. w.f. of hybrid,  $15 \text{ g L}^{-1}$  of  $\text{Na}_2\text{SO}_4$  and three drops of a wetting agent are added to the dyeing bath. The dyeing process is then carried out for 45 min at  $95 \text{ }^\circ\text{C}$  (Fig. 6), obtaining the dyeing of the cotton whose reference will be TCPHA-1. This dyeing process will be repeated but pre-dyeing the cotton fabric described with the mordants (Fig. 6), and variables described in Table 1.

One of the great advantages of this process is that direct dyeing with the dye and with the dye adsorbed on the clay has the same yield. The same results of equalisation, dyeing kinetics, solids, etc. are achieved.

### 2.2.3. Printing

Furthermore, alongside dyeing, printing procedures were also carried out. For this purpose, a pre-prepared printing paste sourced from MagnaPrinti® was used. Specifically, MagnaPrint® AquaFlex V2 Neutral was selected. To imbue the paste with colour, the hybrid pigment was incorporated at a ratio of  $30 \text{ g kg}^{-1}$ . For this colouring a fabric with a grammage of  $135 \text{ g m}^{-2}$ ,  $25 \text{ yarns}\cdot\text{cm}^{-1}$ ,  $22 \text{ weft}\cdot\text{cm}^{-1}$  of plane weave openwork fabric was used. The yarn count in both warp and weft is 35 tex. Subsequent to printing, the material was allowed to dry for 15 min at  $60 \text{ }^\circ\text{C}$  and then subjected to thermofixation at  $165 \text{ }^\circ\text{C}$  for 90 s using an oven. The results were assessed using a Minolta CM-3600d reflection spectrophotometer in accordance with ISO 105-A05:1996

Table 1  
Mordants used and conditions.

Mordant	Con. (o.w.f.)	Bathroom Ratio	Temperature	Time
Alum	2 %	1:10	95	30'
Titanium oxalate	0.8 %			
Aluminium lactate	0.8 %			
Ferric sulphate	0.24 %			

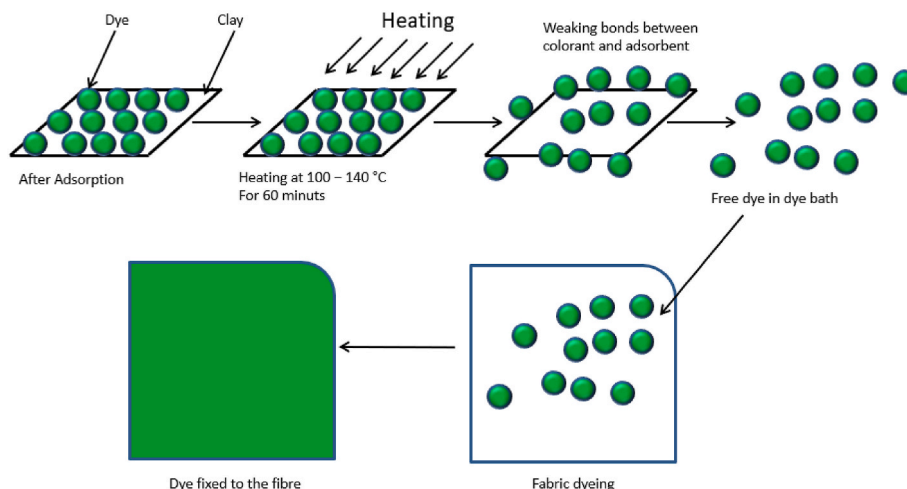


Fig. 5. Dye desorption and dyeing of the textile fibre.

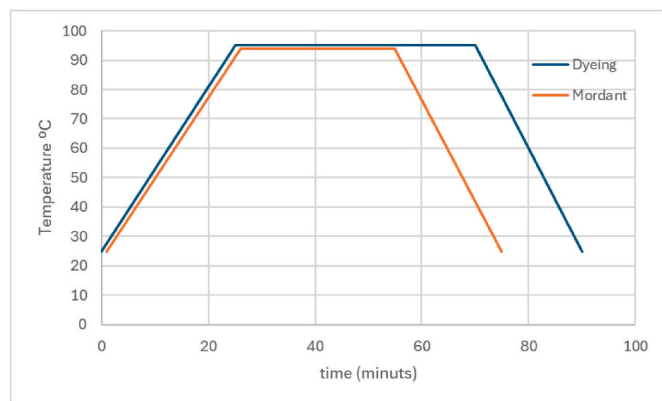


Fig. 6. Dyeing and premordant curve.

Table 2

Samples obtained after staining processes.

Coloration method	Mordant	Reference
Dyeing without mordant	–	TCPHA-1
Dyeing with mordant	Alum	TCPHA-2
Dyeing with mordant	Titanium oxalate	TCPHA-3
Dyeing with mordant	Aluminium lactate	TCPHA-4
Dyeing with mordant	Ferric sulphate	TCPHA-5
Printing	–	SCPHA

standards for subsequent degradation evaluation, yielding CIE tristimulus values for the D65 illuminant and the 10° CIE standard observer. The print sample was referenced as SCPHA. Table 2 shows a summary of the samples obtained after the different staining processes described.

#### 2.2.4. GOTS and NODS criteria

The Natural Organic Dye Standard (NODS) is a set of guidelines and requirements designed to ensure the quality, safety, and environmental sustainability of natural dyes used in textiles. This standard covers the entire lifecycle of the dyeing process, from the cultivation of dye plants to the final application on fabrics. Dyes must be derived from organic materials, such as plants, insects, or minerals, which are cultivated or harvested in ways that promote biodiversity and soil health, avoiding the use of synthetic pesticides and fertilisers. The extraction of dyes must be carried out using environmentally friendly methods, utilizing water and other non-toxic solvents to ensure no harmful chemicals are introduced into the environment [97,98].

The use of chemical additives in the dyeing process is strictly controlled; only those that meet organic standards and pose no risk to human health or the environment are permitted. The entire dyeing process must minimise water and energy consumption, and effluents must be treated to remove any residual chemicals, ensuring that discharged water is clean and safe. Furthermore, the dyes must be non-toxic and safe for consumers, which includes ensuring that dyed textiles do not contain harmful residues that could affect the skin or overall health of users [99–101].

Every stage of the dye production process must be documented and traceable to ensure compliance with NODS, with regular audits and verifications conducted by independent certification bodies.

In contrast, the Global Organic Textile Standard (GOTS) is the leading worldwide standard for organic textiles and covers the entire supply chain, ensuring that textiles are produced in an environmentally and socially responsible manner. Products must contain a minimum of

70 % certified organic fibres, and for products labelled as “organic,” the requirement is 95 %. All processing units must comply with stringent environmental criteria, prohibiting the use of toxic heavy metals, formaldehyde, and genetically modified organisms. Processing must be conducted in a way that reduces environmental impact, including proper waste management and water treatment [102].

GOTS also restricts the use of hazardous chemicals at all stages of production, allowing only approved dyes and auxiliaries that meet specific environmental and toxicological criteria. Additionally, it includes robust social criteria based on key norms of the International Labour Organization, covering workers’ rights, including safe and hygienic working conditions, fair wages, and the prohibition of child labour. The use of sustainable and recyclable packaging materials is encouraged, and products must be clearly labelled to ensure transparency regarding the organic status and certification of the product.

GOTS requires comprehensive testing and quality assurance measures, including residue testing of the final product to ensure it meets specified organic and environmental standards. GOTS certification is conducted by independent, accredited bodies, and regular inspections and audits ensure ongoing compliance with the standard. Traceability and documentation are key components of the certification process.

#### 2.3. Characterization

The quantification of dye adsorption by the nano-clay system was pivotal in determining the efficiency of the synthesis process. Employing a UV–Vis transmission spectrophotometer (JASCO V650, Easton, MD, USA), the absorbance (%) of the dye in distinct supernatants was measured, allowing for the calculation of the amount of dye adsorbed by the nano clays as a percentage of the initial concentration during the exchange phase.

XRD analysis was conducted using Bruker D8-Advance equipment (Bruker, Billerica, MA, USA) equipped with a Göebel mirror (power: 3000 W, voltage: 20–60 kV, current: 5–80 mA). Measurements were performed under oxidant atmosphere conditions at an angular speed of 1°/min, STEP 0.05°, and an angular scan ranging from 2.7° to 70°. XRD patterns were obtained to observe alterations in the basal space of the layers from different nano clays resulting from interactions with the natural dye and modifiers.

For Total Solar Reflectance (TSR) analysis, a double UV–Vis/NIR Jasco V-670 spectrometer operating within the wavelength range from 190 to 2700 nm was utilized [103]. The instrument features a double-grating monochromator, one for the UV–Vis region (1200 grids/mm) and another for the NIR region (300 grids/mm). Automated detector and grating changes occur at a user-defined wavelength between 750 and 900 nm. Light sources include a deuterium lamp (190–350 nm) and a halogen lamp (330–2700 nm). Optical properties were calculated using reflectance factors  $p(\lambda)$  for hybrid pigments within the 370–740 nm range with the D65 illuminant and the CIE-1964 standard observer [18].

To assess the thermal characteristics of the hybrid, a thermogravimetric analysis of chlorophyll in nano clay was carried out using a TGA/SDTA 851 (Mettler-Toledo Inc., Columbus, OH, USA). Experimental conditions involved a temperature ramp of 5 °C/min within the 20–900 °C range under an oxidant medium of N<sub>2</sub>:O<sub>2</sub> (4:1) [104–106].

The surfaces of the samples underwent topographical analysis using a scanning electron microscope (SEM), specifically the PHENOM model (FEI Company, Eindhoven, The Netherlands), operated at an electron acceleration of 5 kV. Prior to analysis, a coating of gold-palladium alloy (5–7 nm thickness) was applied to the samples using an EMITECH sputter coater model SC7620 (Quorum Technologies Ltd., East Sussex, UK).

For characterization purposes, Fourier transform infrared spectrophotometry (FTIR) was performed utilizing a horizontal attenuated total reflection (FTIR-ATR) configuration with a ZnSe prism on a Jasco FTIR 4700 IRT 5200 spectrometer equipped with a DTGS detector. The spectrum was generated through 64 scans at a resolution of  $4\text{ cm}^{-1}$ .

Energy dispersive X-ray (EDX) analyses were conducted using a JEOL JSM-6300 scanning electron microscope. To ensure conductivity of non-conductive surfaces, all samples underwent pre-coating with graphite. The choice of non-metallic coatings was deliberate to mitigate potential interferences in the results. The acquired EDX spectra facilitated the determination of elemental composition of the materials deposited onto the hybrid surfaces.

The BET analysis was performed to determine the surface area, pore volume, and pore size using nitrogen adsorption and desorption data at  $-196\text{ }^\circ\text{C}$ , using a Micromeritics ASAP-2020 instrument. Prior to analysis, the samples underwent degassing under a vacuum atmosphere within the temperature range of  $150\text{ }^\circ\text{C}$ – $200\text{ }^\circ\text{C}$  to prevent any carbonization of sample constituents [107,108].

### 3. Results and discussion

Halloysite, a naturally occurring nanotubular clay, is emerging as an effective adsorbent for the natural dye chlorophyll due to its unique structure and surface properties. Its nanotubes have a high surface area to volume ratio, which increases their adsorption capacity. In addition, the inherent negative surface charge of halloysite facilitates interaction with the cationic dyes present in chlorophyll, thus improving their adsorption efficiency. The tubular morphology of halloysite also provides accessible active sites for the capture of dye molecules, ensuring effective and selective adsorption of chlorophyll. In addition, its abundance, low cost and biocompatible nature make it a promising option for the purification of natural dyes. Halloysite not only offers a sustainable alternative to conventional adsorbents, but also opens new possibilities in applications related to the removal and recovery of natural dyes, thus contributing to the improvement of environmental quality and sustainability in a number of industries.

#### 3.1. Final concentration in solution

After the adsorption and centrifugation process to separate the hybrid from the supernatants water, the supernatants water was analysed to evaluate the percentage of dye adsorption by the HA. The results were 98 % adsorption with a standard deviation of 1.87, thus proving the adsorption capacity of the halloysite for the dye studied. The calculation of the amount of dye in the supernatant water was carried out using the Lambert-Beer equation previously performed for the chlorophyll dye (Fig. 7).

#### 3.2. Hybrid colour measurements and TSR(%)

Table 3 and Fig. 8 show the measurements made to determine the colour of the hybrid obtained and of the clay prior to the synthesis process, as illustrated in the colour chart. The primary colour calculations for each hybrid pigment were determined using the reflectance values ( $\lambda$ ) of these dye-HA hybrids, following the principles established by the International Commission on Illumination CIE 15:2004 [109]. These guidelines enable a fair comparison of both absolute and relative colour values by applying CIELAB colorimetric parameters, according to

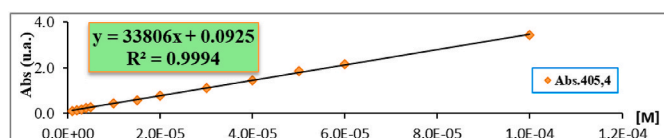


Fig. 7. Lamber-Beer equation for the dye Copper chlorophyll.

Table 3

$L^*$ ,  $a^*$ ,  $b^*$ ,  $C^*_{ab}$ ,  $h$  and TSR values of hybrid and halloysite.

Sample	$L^*$	$a^*$	$b^*$	$C^*_{ab}$	$h_{ab}(\text{deg})$	TSR(%)
HA	88.201	0.070	1.544	1.545	87.397	70.569
CPHA	66.587	-8.804	7.368	11.480	140.075	45.979

the CIE 1931 XYZ standard and the D65 standard illumination. The diagram of CIE  $a^*b^*$  and CIE- $Cab^*L^*$  depicted in Fig. 8 confirm the successful sequestration of the dye extracted from the solution within the nano-adsorbent. This is evidenced by the manifestation of colours that are characteristic of the resulting pigments. The hybrid obtained shows a somewhat yellowish green hue with high saturation values considering that a rather dark sample is obtained, with a lightness level  $L^*$  which does not reach a value of 70.

Total solar reflectance is a fundamental parameter in the study of how solar radiation interacts with land surfaces. This term refers to the ability of a material to reflect incident solar radiation at all wavelengths, which is crucial for understanding thermal and energetic effects in both man-made and natural environments.

When solar radiation reaches a surface, some is absorbed, some is transmitted through the material and the rest is reflected. Total solar reflectance is expressed as a percentage representing the fraction of the total solar radiation that is reflected by the material. Materials with high total solar reflectance tend to reflect more sunlight and therefore absorb less heat, which helps to reduce heat gain in structures and pavements.

This concept is particularly important in the design of sustainable urban environments and in the energy efficiency of buildings. Surfaces with high total solar reflectance, such as reflective roofs and pavements, can help mitigate the urban heat island effect by reducing heat absorption and improve the energy efficiency of buildings by reducing the need for cooling.

When assessing the performance and resistance of coatings such as textile printing pastes to external surfaces, the total solar reflectance factor (TSR) becomes crucially important. TSR measures the ability of a material to reflect incident solar radiation as a percentage of the total radiation incident on its surface. High TSR values indicate effective reflection of solar radiation, which reduces heat absorption and surface temperatures. Calculated by solar reflectance measurements at various wavelengths, TSR considers the entire solar spectrum, adjusted by solar weighting factors that adapt the spectral distribution. TSR is especially significant in applications such as roof coverings and solar shading fabrics, where minimising heat absorption is essential for energy efficiency.

A higher TSR contributes to lower surface temperatures and decreased cooling loads. These calculations adhere to ASTM G173-03 [110] guidelines, providing a standardized approach to evaluating materials in diverse applications. Table 3 shows the TSR results obtained for the synthesized hybrid and the pure form HA before dye adsorption. Initially, the nano clay has a much higher  $L^*$  luminosity than the resulting hybrid, as can be seen in Table 3. As a result, elements with a lower TSR have surfaces with higher temperatures than those of halloysite alone.

Fig. 9 shows the reflectivity spectra of the 8 hybrids and laponite. The analysis of this spectrum can be performed in 4 zones, the ultraviolet (200–400 nm), the visible (400–700 nm), the near infrared (700–1200 nm) and the infrared (1200–2400 nm). The HA alone has a much higher reflectivity in the UV, visible and near-infrared regions, i.e. between 200 and 1200 nm. However, from wavelengths above 1200 nm, the intensity of the halloysite reflectance begins to attenuate, reaching values very similar to the hybrid CPHA.

From the wavelengths in the near infrared, the reflectances recorded are those produced by the specific chemical groups in the samples studied. In our case and as seen in the FTIR analysis, the clay bands largely cover those of the dye, which is why in Fig. 8 in the NIR zone both bands are very similar.

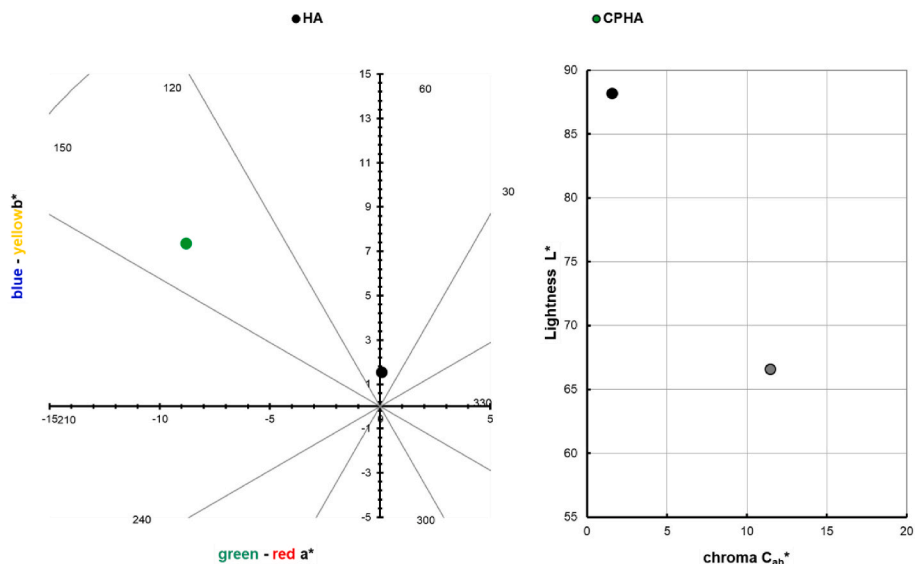


Fig. 8. Graphic CIELAB plots for hybrid pigments synthesized, including the clay (HA) using the D65 illuminant and the CIE-1931 XYZ standard observer. Left: CIE-a\*b\* colour diagram; right: CIE-Cab\*L\* colour chart.

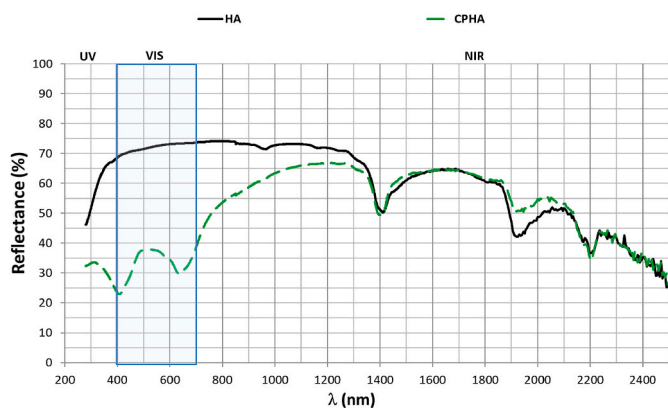


Fig. 9. Reflectance of hybrid CPHA and HA.

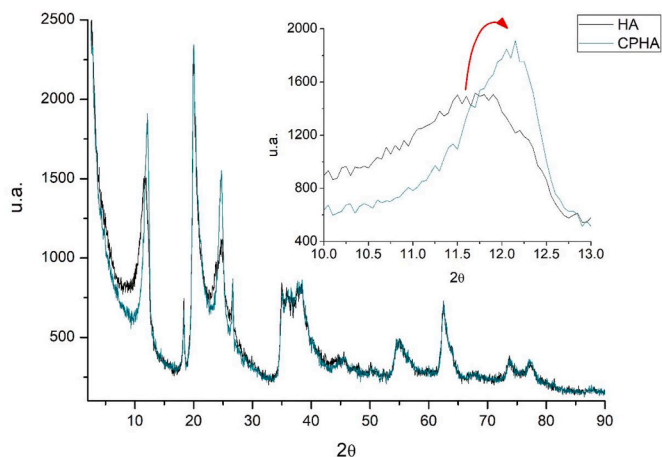


Fig. 11. XRD for Halloysite and hybrid CPHA.

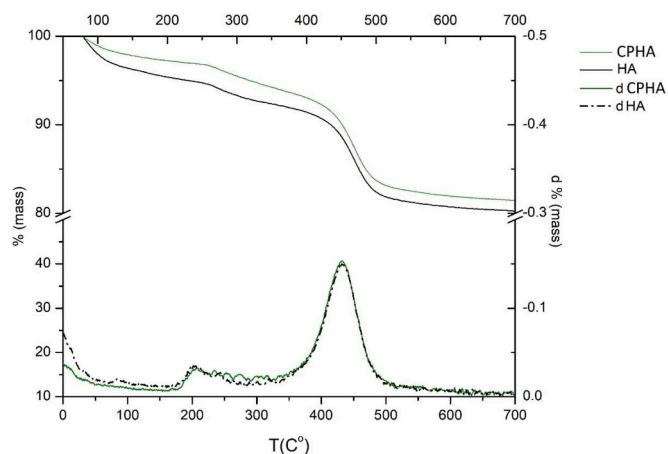


Fig. 10. TGA and DTGA of hybrid CPHA and HA.

### 3.3. Thermogravimetry (TGA-DTGA)

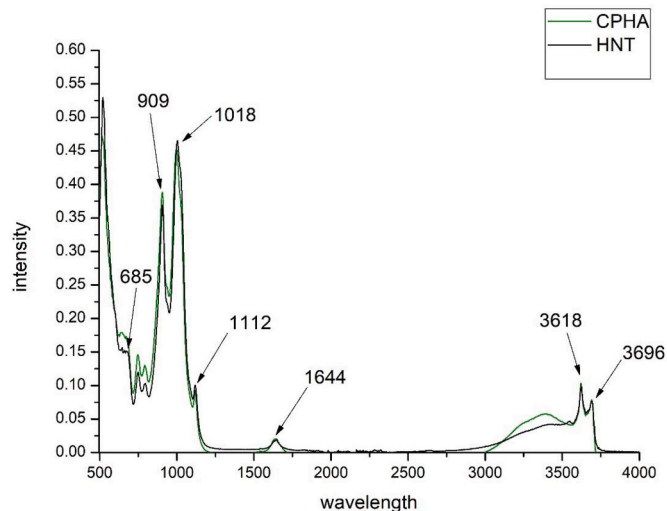
Thermal analyses were conducted by evaluating the mass loss across specific temperature ranges and examining the derivative curves to compare the peaks of maximum degradation. Thermograms were

carried out for both the original nano clay and the hybrid pigment CPHA (Fig. 10). However, in the hybrid pigment, it was difficult to identify peaks corresponding to the thermal degradation of the chlorophyll dye due to the noise present and the greater effect of the nano clay. A reduced desorption of H<sub>2</sub>O could only be observed in the hybrid pigment, which was attributed to water substitution during the synthesis process. According to the literature [111,112], the two weight losses observed in halloysite could be associated with H<sub>2</sub>O loss and dehydroxylation of the halloysite matrix. The first peak, related to H<sub>2</sub>O loss and detected before reaching 100 °C, showed a significant decrease in the CPHA hybrid sample. Differential thermogravimetric analysis (DTGA) revealed mild endothermic and marked exothermic behaviour at 100 °C and 300 °C, respectively, which agrees with the data obtained by thermogravimetric analysis (TGA). This behaviour indicated physical desorption of adsorbed water at 100 °C and oxidative desorption of the organic compound (chlorophyll) between 300 °C and 400 °C [113]. Therefore, it can be concluded that the hybrid sample exhibits a good thermal stability up to 300 °C.

**Table 4**

Calculated interlaminar spacing  $d(001)$ nm for halloysite and synthesized pigment CPHA.

Sample	$2\theta$	$\theta$ ( $^\circ$ )	$\theta$ (rad)	$d(001)$ Å	$d(001)$ nm
HA	11.70	5.85	0.10	7.56	0.756
CPHA	12.10	6.05	0.11	7.31	0.73

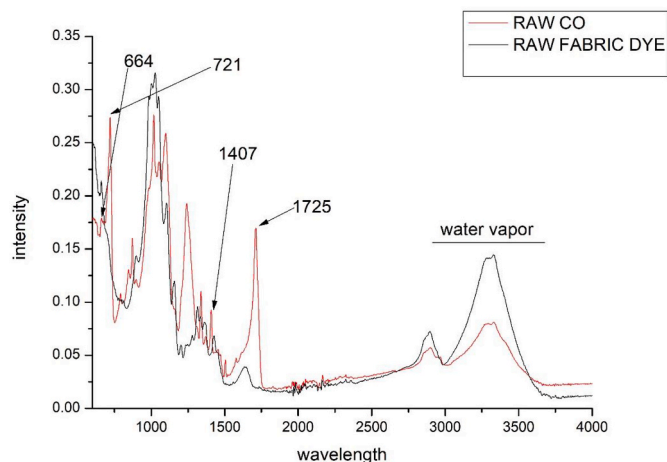
**Fig. 12.** FTIR-ATR Halloysite and hybrid CPHA.

### 3.4. X-ray diffraction (XRD)

The XRD analysis (Fig. 11 and Table 4) of the hybrid formed by halloysite revealed characteristic peaks at  $2\theta = 8^\circ, 13^\circ, 22.8^\circ, 28^\circ, 31^\circ, 58^\circ,$  and  $67^\circ$  [114,115]. With these samples, the initial halloysite peak was noted at  $11.5^\circ$ , which subsequently shifted to  $12.3^\circ$ . This shift indicated a reduction in the  $d_{001}$  peak spacing from the original 0.756 nm in the pure nano-adsorbent to 0.730 nm in the hybrid sample, suggesting compression of the clay layers due to organic loading under synthesis conditions. Notably, there were no significant discrepancies observed in the factors identified throughout the analysis.

### 3.5. Fourier transform infrared spectroscopy FTIR-ATR analysis

Fig. 12 shows the spectra of the FTIR-ATR analysis of the raw halloysite samples and the hybrid formed by the nano clay and the adsorbed

**Fig. 13.** FTIR Co fabric raw and Dyed fabric raw.**Table 5**

EDX values for sample CPHA.

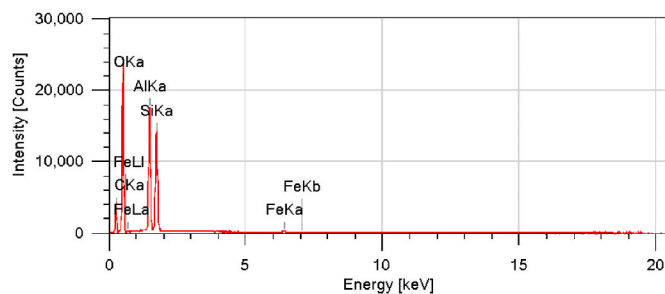
Element	Mass%	Atom%
C	$21.82 \pm 0.06$	$29.97 \pm 0.09$
O	$54.20 \pm 0.12$	$55.87 \pm 0.12$
Al	$12.13 \pm 0.04$	$7.42 \pm 0.02$
Si	$11.11 \pm 0.04$	$6.52 \pm 0.02$
Fe	$0.74 \pm 0.02$	$0.22 \pm 0.01$

chlorophyll dye. As can be seen in the figure, both spectra are practically superimposed, as it is the clay that has all the prominence and covers the spectra formed by the vibrations that may be produced by the chlorophyll. The vibration bands are displayed as follows: the bands located at  $3696$  and  $3618 \text{ cm}^{-1}$  are attributed to two  $\text{Al}_2\text{OH}$ -stretching bands (with each OH group linked to two Al atoms) [116–118]. In the spectrum, a peak at  $1644 \text{ cm}^{-1}$  is detected, indicating highly pronounced bending vibrations of the adsorbed water [119]. The peak at  $1112 \text{ cm}^{-1}$  is attributed to apical Si–O bonds [116,120]. The peaks at  $1018$  and  $685 \text{ cm}^{-1}$  are attributed to perpendicular stretching vibrations of Si–O–Si bonds [119]. The band detected at  $909 \text{ cm}^{-1}$  arises from the O–H deformation of inner hydroxyl groups [116,120].

Studying Fig. 13, a peak at  $1725 \text{ cm}^{-1}$  is attributed to asymmetric stretching vibration of the carbonyl band [121]. At  $664, 721$  and  $1407 \text{ cm}^{-1}$  several peaks are seen corresponding to carbon dioxide  $\text{CO}_2$ , acetylene  $\text{C}_2\text{H}_2$  and propylene  $\text{C}_3\text{H}_6$  respectively [121]. The area between  $300$  and  $3700 \text{ cm}^{-1}$  is given by water vapour. Many of the bands described lose intensity in the sample after dyeing, as can be seen in the graph in Fig. 13.

### 3.6. Scanning electron microscopy energy + dispersive X-ray spectroscopy (SEM-EDX)

Energy dispersive X-ray spectroscopy (EDX) was used to conduct an analysis of the hybrid surface, with the aim of confirming the constituent elements present in the CPHA hybrid (Table 5, and Fig. 14), Co fabric raw (Table 6 and Fig. 15), and fabric dyed raw (Table 7 and Fig. 16). The spectra resulting from this analysis are depicted in Fig. 14. In addition, Table 5 shows the mass and percentages of atoms of each element detected. In these spectra, characteristic peaks are observed at  $0.37, 0.41, 0.49, 1.44,$  and  $1.83 \text{ keV}$  corresponding to the elements Fe, C, O, Al, Si respectively. In addition, other peaks corresponding to iron can be seen at  $6.21$  and  $7.08 \text{ keV}$ .

**Fig. 14.** EDX for sample CPHA.**Table 6**

EDX values for Co fabric raw.

Element	Mass%	Atom%
C	$38.73 \pm 0.20$	$45.85 \pm 0.24$
O	$60.61 \pm 0.41$	$53.86 \pm 0.37$
Al	$0.10 \pm 0.02$	$0.05 \pm 0.01$
Na	$0.12 \pm 0.03$	$0.07 \pm 0.02$
K	$0.44 \pm 0.03$	$0.16 \pm 0.01$



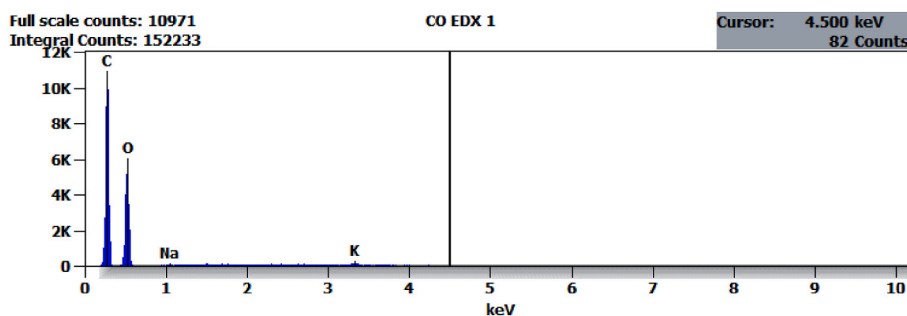


Fig. 15. EDX for Co fabric raw.

Table 7

EDX values for fabric dyed raw.

Element	Mass%	Atom%
C	34.00 ± 0.18	40.91 ± 0.21
O	64.72 ± 0.39	58.46 ± 0.35
Si	1.11 ± 0.03	0.57 ± 0.02
Ca	0.17 ± 0.02	0.06 ± 0.01

As in the FTIR analysis described above, no peaks of elements characteristic of chlorophyll are observed. Again, the HA bands cover the possible peaks that could be present in chlorophyll elements such as copper. Given that both analyses give this information, it can be assumed that the dye has been deposited inside the halloysite nanotubes, not allowing readings of its elements to be obtained by surface analysis such as EDX and FTIR-ATR. It is worth pointing out that the inner layer of the halloysite is positive and the outer layer negative, the dye in aqueous solution is negative, so the dye must be housed inside the nanotube because of its charge. Nevertheless, the presence of the dye is evident given the colour obtained by the hybrid, which could not be obtained if it were not for the adsorption of the dye.

### 3.7. Brunauer–Emmett–Teller (BET) surface area and porosity measurements

A thorough BET analysis was conducted to examine the surface properties of the clay, along with the dimensions and depth of its respective pores, as outlined in Table 8. A comparative assessment was undertaken between the halloysite sample prior to adsorption and after dye adsorption. The findings collated in Table 8 reveal noteworthy alterations in both pore size and depth after adsorption. This is because when the halloysite comes into contact with the dye, the chlorophyll molecules adhere to its surface by adsorption forces. As the chlorophyll molecules accumulate on the surface of the halloysite, they occupy part of the internal pore space of the mineral.

This process of chlorophyll adsorption leads to a decrease in the

Table 8

BET surface areas, pore volumes and average pore sizes for Halloysite (HA), and hybrid CPHA.

Sample	Surface area (m <sup>2</sup> /g)	Pore volume (cm <sup>3</sup> /g)	Average pore size (nm)
HA	180.3	0.21	10.07
CPHA	47.6	0.11	8.7

volume and surface area of the halloysite pores. As the pores fill with dye molecules, less space is available within the clay structure for additional adsorption of other substances. Therefore, the ability of halloysite to adsorb other molecules is reduced, and its effective pore volume and surface area decrease after chlorophyll dye adsorption.

### 3.8. Measurement of printing and dyeing colour

The primary aim of this study was to attain textile material colouring through the printing technique using hybrids derived from halloysite as the pigment agent, and by means of exhaustion dyeing using these HA hybrids as the dyeing material. Following the accomplishment of this objective, the coloration of the textile substrate was quantified and assessed. The L\*a\*b\* h and C\*ab values have been tabulated in Table 9 and depicted in a chromaticity diagram in Fig. 17, demonstrating the successful attainment of the set objective.

Clear differences can be seen between the samples with mordant and those without in the dyes. The samples with mordant are less yellowish than the one without mordant but their hue is less pure and less saturated, as can be seen in the chroma level C obtained. The sample without mordant is somewhat darker than those with any type of mordant. Also significant is the effect of iron sulphate, which negatively affects the hue of the original dye, changing it completely to a reddish-brown tone. So, despite being the most chromatic and darkest sample, the use of this mordant would be inadvisable if green tones are to be obtained with this kind of hybrid.

Among the rest of the mordants there is little difference in terms of hue, or the saturation and clarity obtained, however, Titanium oxalate and Aluminium lactate are more interesting with darker and more

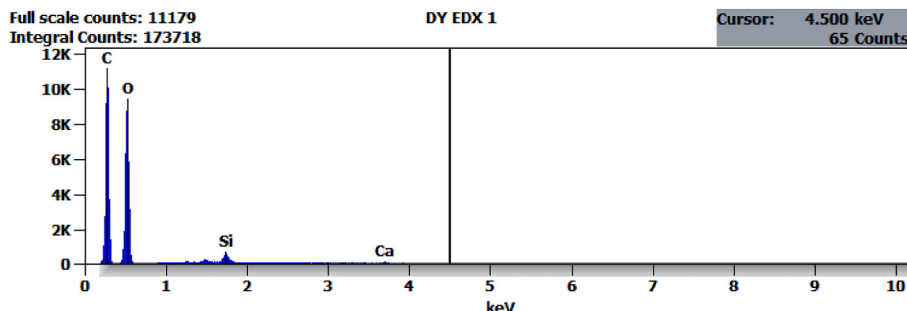








Fig. 16. EDX for fabric dyed raw.

**Table 9**

L\*, a\*, b\*, C\*ab values of each printing and dyeing.

Sample	Dye Shade	L *	a *	b *	C * <sub>ab</sub>	h	K/S (average)	ΔE
Raw		82.72	0.88	-4.56	4.65	281.01	-	-
TCPHA-1		74.45	-9.18	12.49	15.50	126.32	1.2582	74.53
TCPHA-2		75.44	-6.25	11.34	12.95	118.86	0.3349	75.84
TCPHA-3		78.40	-5.41	10.47	11.79	117.33	0.3545	81.65
TCPHA-4		76.06	-6.58	11.00	12.82	120.89	0.4692	61.39
TCPHA-5		65.16	3.89	24.94	25.24	81.13	0.3640	114.68
SCPHA		77.82	-7.31	8.49	11.20	130.73	1.2531	82.85

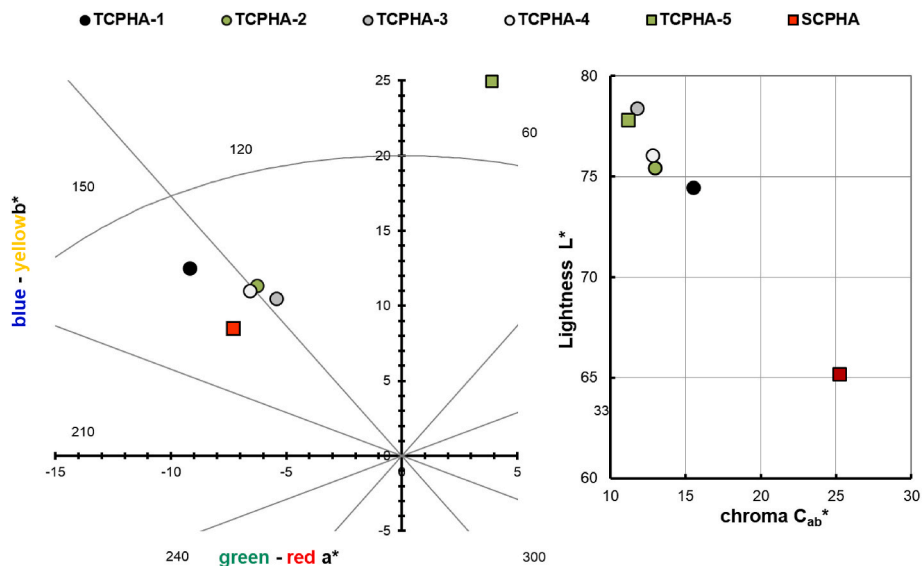


Fig. 17. Representation of the chromatic coordinates for each of the colour samples of the cotton fabrics.

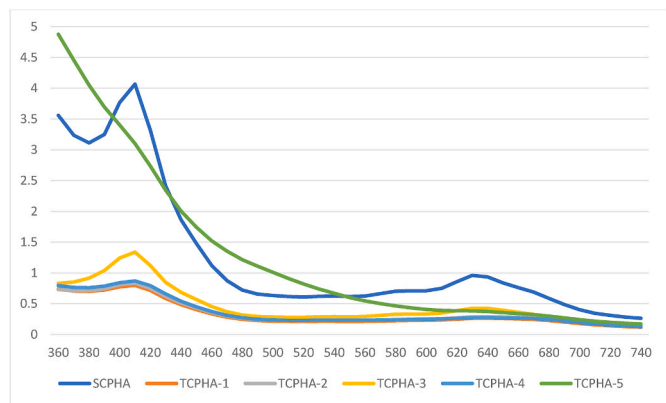


Fig. 18. K/S spectra (360–740 nm) for each sample.

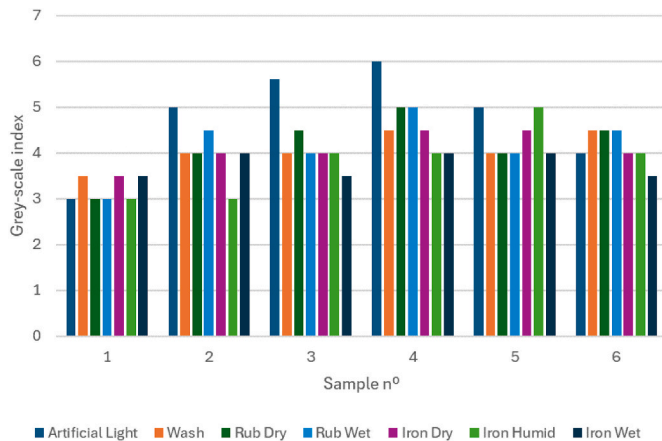
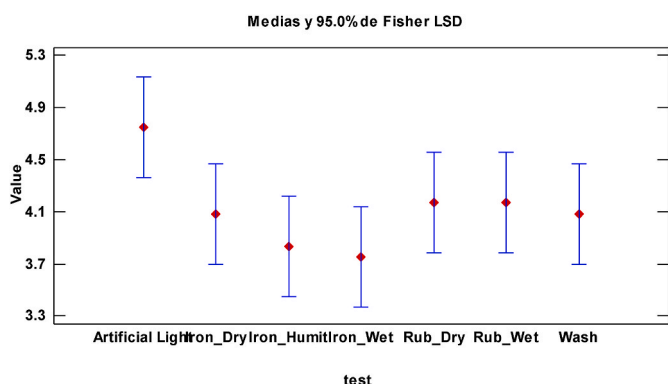


Fig. 19. Comparison of colour fastness values by grey-scale index.

**Table 10**  
Colour Fastness for each sample.

Sample n°	Reference	Colour Fastness						
		Artificial Light	Wash	Rub		Iron		
				Dry	Wet	Dry	Humid	Wet
1	TCPHA-1	3	3–4	3	3	3–4	3	3–4
2	TCPHA-2	5	4	4	4–5	4	3	4
3	TCPHA-3	5–6	4	4–5	4	4	4	3–4
4	TCPHA-4	6	4–5	5	5	4–5	4	4
5	TCPHA-5	5	4	4	4	4–5	5	4
6	SCPHA	4	4–5	4–5	4–5	4	4	3–4



**Fig. 20.** LSD Fisher means plot (95 %) for the comparison of the grayscale value with different tests for colour fastness.

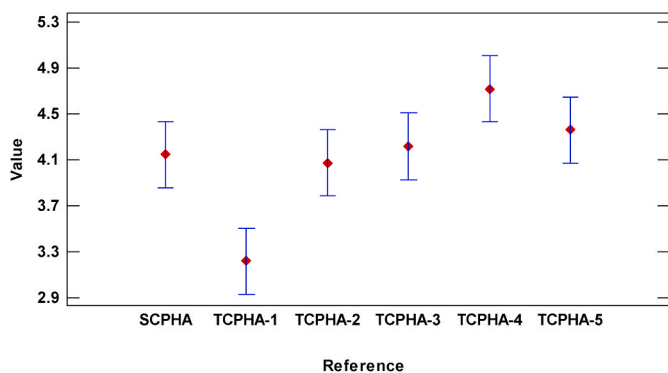


**Fig. 21.** LSD Fisher means plot (95 %) for the comparison of the grayscale value with different textile applications.

saturated colours. As expected in the printing a much more intense colour is obtained more saturated and darker than when dyeing in terms of covering power.

Furthermore, an analysis was carried out of the intensity or strength of the colour obtained in each colouring sample, both dyeing and printing. This colour strength has been calculated by means of the K/S. These average [122,123] values are shown in Table 9 and the spectra in Fig. 18. The samples with the most intense colour are those of TCPHA-1, TCPHA-5 and SCPHA, although the TCPHA-5 sample has a significant colour alteration due to the effect of the mordant (see Fig. 19).

### 3.9. Colour fastness

Once the objective of colouring various textile materials with nano

clays imbued with dyes has been attained, it becomes imperative to verify the longevity of these colours on the substrates over time, despite exposure to various external factors causing wear and tear. With this in mind, a series of colour fastness tests were conducted on the hybrid colours. Table 10 presents the results obtained from each of these distinct colour fastness tests. These results are depicted based on the standard greyscale (GSc) and determined instrumentally via Equation 1 following the UNE-EN ISO 105-A05 guidelines. Visual assessment based on a blue scale was carried out for the artificial light and weathering colour degradation tests.

$$a) \Delta E_F = [(\Delta L^*)^2 + (\Delta C_I)^2 + (\Delta H_I)^2]^{1/2}$$

$$b) GS = 5 - [\Delta E_F / 1.7]$$

$$c) GS = 5 - [\log_{10} (\Delta E_F / 0.85) / \log_{10} 2]$$

**Equation 1.** a) Colour change for the determination of the greyscale index for degradation b) GS if  $\Delta E_F \leq$

Analysing the results of the fastnesses and comparing them with those obtained in other works published by the scientific community [124–127], on the one hand, the results obtained by printing are quite good, since the lowest value is 3–4 for wet ironing, which is a quite acceptable result, and this reaches 4–5 in different tests such as washing and rubbing. Therefore, printing with hybrid nanopigment can be considered successful.

On the other hand, analysing the results of the dyeing, that the results show that the dyeing of the cotton fabric without any type of TCPHA-1 mordant is the one with the lowest fastness values. With all the mordants used, improvements in fastnesses have been achieved, especially the results obtained with Aluminium lactate, which shows the best results. In addition, the dyeing using this same mordant has also had very good results as can be seen in the analysis in section 3.10 Measurement of printing and dyeing colour.

In this case, the ANOVA technique was used to determine if the type of technique used for the application of colour, dyeing with different mordants or printing, obtained statistically significant differences in terms of fastness. This technique was also used to determine if, independently of the application, the hybrids obtained statistically significant differences according to the test to which they were submitted. In both cases statistically significant differences were obtained (P-Value lower than  $\alpha = 0.05$ ). Firstly, regardless of the application conditions, the fastnesses are higher with artificial light, while they decrease when humidity is involved (Fig. 20).

Secondly, according to the type of application, significant differences were also observed regardless of the type of test to which the samples were subjected. In this case, the worst results are obtained without the mordant, which was to be expected since this compound is used to improve fastness, demonstrating its effectiveness here. There are significant differences between the mordants, with the best results shown

by the Aluminium Lactate, followed by the Ferric Sulphate, which is discarded because of the tone. Then the Alum and Titanium Oxalate gets the same results as the stamped sample (Fig. 21).



#### 4. Conclusions

The utilization of halloysite, a naturally occurring nanotubular clay, as an adsorbent for the natural dye chlorophyll has been demonstrated to be highly effective. This effectiveness stems from the unique structural and surface properties of halloysite, which enable efficient adsorption of chlorophyll molecules. This study uses the NODS-compliant dye copper chlorophyll as the chlorophyll is obtained from NODS-listed plants such as *Chlorophora tinctoria*, *Chlorophora affinis* or *Chlorophora braziliensis*. It could therefore be scaled up to an industrial level without the dye being a limitation.

The high surface area to volume ratio of halloysite nanotubes enhances their adsorption capacity, while the inherent negative surface charge facilitates interaction with cationic dyes present in chlorophyll, thereby improving adsorption efficiency. Additionally, the tubular morphology of halloysite provides accessible active sites for the capture of dye molecules, ensuring effective and selective adsorption of chlorophyll. Moreover, the abundance, low cost, and biocompatible nature of halloysite make it a promising option for the purification of natural dyes, offering a sustainable alternative to conventional adsorbents. Besides, chlorophyll is very sensitive and must be stored at low temperatures, but by encapsulating it in clay it is protected and cold storage is not necessary. In addition, encapsulation/trapping can be used as a means of dye recovery in textile wastewater.

Experimental results confirm the efficacy of halloysite in adsorbing chlorophyll, with a remarkable adsorption capacity of 98 %. Characterization techniques such as X-ray diffraction (XRD), Fourier transform infrared spectroscopy (FTIR), scanning electron microscopy energy dispersive X-ray spectroscopy (SEM-EDX), thermogravimetry (TGA), and Brunauer–Emmett–Teller (BET) surface area and porosity measurements provide insights into the structural changes and interactions occurring during the adsorption process. These analyses reveal the successful sequestration of chlorophyll within halloysite nanotubes, evidenced by shifts in characteristic peaks and the absence of chlorophyll-specific elements in surface analyses.

Furthermore, colorimetric assessments and total solar reflectance (TSR) measurements demonstrate the practical implications of halloysite-based adsorption in textile applications and urban design. The synthesized hybrid pigments exhibit distinct coloration, confirming the retention and manifestation of chlorophyll within the halloysite matrix. Moreover, the reduction in total solar reflectance after dye adsorption highlights the potential of halloysite in modifying surface properties for energy-efficient coatings and urban heat island mitigation.

Overall, this comprehensive study underscores the promising role of halloysite as an effective adsorbent for natural dyes, with implications for environmental improvements, sustainable manufacturing, and urban sustainability. The successful adsorption of chlorophyll onto halloysite nanotubes not only expands our understanding of clay-based adsorbents but also opens avenues for innovative applications in diverse fields,

contributing to the advancement of environmental quality and sustainability initiatives.

#### CRediT authorship contribution statement

**Daniel López-Rodríguez:** Writing – original draft, Methodology, Investigation, Formal analysis, Conceptualization. **Jorge Jordan-Núñez:** Software, Project administration, Funding acquisition, Conceptualization. **Bàrbara Micó-Vicent:** Writing – review & editing, Validation, Supervision, Methodology. **Antonio Belda:** Resources, Investigation, Formal analysis, Conceptualization.

#### Declaration of competing interest

The authors declare that they have no known competing financial interests or personal relationships that could have appeared to influence the work reported in this paper.

#### Data availability

No data was used for the research described in the article.

#### Acknowledgment

To the Vice-rectorate for research of the UPV for Funding for open access charge: CRUE-Universitat Politècnica de València.

The project ‘Microbiomat: R + D new dyes for application in vegetable textiles and alternative biomaterials to leather to obtain products for the fashion sector’ is financed by the Valencian Agency for Innovation through the Strategic Projects programme with file number INN-EST/2022/214 and is made up of the following consortium José Gisbert S.L. Perchados Textiles S.A., Guerola S.A., Mapelor S.L., Acabados Pegasa S.L. and UPV.

#### References

- [1] Kuo Lopin, Chang Bao-Guang. The affecting factors of circular economy information and its impact on corporate economic sustainability-Evidence from China. *Sustain Prod Consum* 2021;27:986–97.
- [2] Bechtold,Thomas; and Rita Mussak; Handbook of natural colorants, vol. vol. 8. John Wiley & Sons..
- [3] Micó-Vicent Bàrbara, et al. Effect of lemon waste natural dye and essential oil loaded into laminar nanoclays on thermomechanical and color properties of polyester based bionanocomposites. *Polymers* 2020;12(7):1–22. <https://doi.org/10.3390/polym12071451>.
- [4] Ozdemir Muge Burcu, Karadag Recep. Madder (*Rubia tinctorum* L.) as an economic factor under sustainability goals in the textile dyeing. *J Nat Fibers* 2023;20(1):2128968.
- [5] Ozdemir Muge Burcu, Karadag Recep. Anatolian acorn oak’s economic potential in the application to the textile and leather industries, vol. 6; 2023. p. 320–32.
- [6] Shalini S, Prasanna S, Mallick Tapas K, Senthilarasu S. Review on natural dye sensitized solar cells: operation, materials and methods. *Renew Sustain Energy Rev* 2015;51:1306–25.
- [7] Heinonen Jari, Farahmandazad Hengameh, Vuorinen Anssi, Kallio Heikki, Yang Baoru, Sainio Tuomo. Extraction and purification of anthocyanins from purple-fleshed potato. *Food Bioprod Process* 2016;99:136–46.

- [8] Keppler Katrin, Hans-Ulrich Humpf. Metabolism of anthocyanins and their phenolic degradation products by the intestinal microflora. *Bioorg Med Chem* 2005;13(17):5195–205.
- [9] Taniguchi Masahiko, Lindsey Jonathan S. Synthetic chlorins, possible surrogates for chlorophylls, prepared by derivatization of porphyrins. *Chem Rev* 2017;117(2):344–535.
- [10] Samanta Ashis Kumar, Agarwal Priti. Application of natural dyes on textiles. 2009.
- [11] Prabhu KH, Bhute Aniket S. Plant based natural dyes and mordants: a Review. *J Nat Prod Plant Resour* 2012;2(6):649–64.
- [12] Singh Rajni, Jain Astha, Panwar Shikha, Gupta Deepti, Khare SK. Antimicrobial activity of some natural dyes. *Dyes Pigments* 2005;66(2):99–102.
- [13] Chengaiah B, Mallikarjuna Rao K, Mahesh Kumar K, Alagusundaram M, Madhusudhana Chetty C. Medicinal importance of natural dyes-a review. *Int. J. PharmTech Res.* 2010;2(1):144–54.
- [14] Sm Gawish, Helmy HM. UV protection properties of cotton, wool, silk and nylon fabrics dyed with red onion peel, madder and chamomile extracts. *J Textil Sci Eng* 2016;6(4). <https://doi.org/10.4172/2165-8064.1000266>.
- [15] Mandal Riddhipratim, Dutta Gorachand. From photosynthesis to biosensing: chlorophyll proves to be a versatile molecule. *Sensors Int* 2020;1:100058.
- [16] Dhafina Wan Almaz, Daud Muhamad Zalani, Salleh Hasiah. The sensitization effect of anthocyanin and chlorophyll dyes on optical and photovoltaic properties of zinc oxide based dye-sensitized solar cells. *Optik* 2020;207:163808.
- [17] Nan Hui, Shen He-Ping, Wang Gang, Xie Shou-Dong, Yang Gui-Jun, Lin Hong. Studies on the optical and photoelectric properties of anthocyanin and chlorophyll as natural co-sensitizers in dye sensitized solar cell. *Opt Mater* 2017; 73:172–8.
- [18] Natale,Corrado Di, Monti Donato, Paolesse Roberto. Chemical sensitivity of porphyrin assemblies. *Mater Today* 2010;13(7–8):46–52.
- [19] Anastopoulos Ioannis, et al. A review on halloysite-based adsorbents to remove pollutants in water and wastewater. *J Mol Liq* 2018;269:855–68.
- [20] Papoulis Dimitrios. Halloysite based nanocomposites and photocatalysis: a Review. *Appl Clay Sci* 2019;168:164–74.
- [21] Ngulube Tholiso, Ray Gumbo Jabulani, Masindi Vhahangwele, Maity Arjun. Evaluation of the efficacy of halloysite nanotubes in the removal of acidic and basic dyes from aqueous solution. *Clay Miner* 2019;54(2):197–207.
- [22] Gabriela Arroyo-Figueroa, Ruiz-Aguilar Graciela ML, German Cuevas-Rodríguez, Gonzalez Sanchez Guillermo. Cotton fabric dyeing with cochineal extract: influence of mordant concentration. *Color Technol* 2011;127(1):39–46.
- [23] Uddin Mohammad Gias. Effects of different mordants on silk fabric dyed with onion outer skin extracts. *J. Text.* 2014;2014.
- [24] Moniruzzaman Md, Mondal Moni Sankar, Hossain Md Nazmul. The influence of mordant and mordanting techniques on ecofriendly dyeing of cotton fabric by extracted used tea. *J Eng Sci* 2018;9(1):111–7.
- [25] Ding Yi, Freeman Harold S. Mordant dye application on cotton: optimisation and combination with natural dyes. *Color Technol* 2017;133(5):369–75.
- [26] Fallisnur F, Sofyan S, Kasim Anwar, Angraini Tuty. Study of cotton fabric dyeing process with some mordant methods by using gambier (Uncaria gambir Roxb) extract. *Int J Adv Sci Eng Inf Technol* 2018;8(4):1098–104.
- [27] Gould Simon WJ, Fielder Mark D, Kelly Alison F, Morgan Marina, Kenny Jackie, Naughton Declan P. The antimicrobial properties of copper surfaces against a range of important nosocomial pathogens. *Ann Microbiol* 2009;59:151–6.
- [28] Vincent M, Duval Raphaël E, Hartemann P, Engels-Deutsch M. Contact killing and antimicrobial properties of copper. *J Appl Microbiol* 2018;124(5):1032–46.
- [29] Usman Muhammad Sani, El Zowalaty Mohamed Ezzat, Shameli Kamyar, Zainuddin Norhazlin, Mohamed Salama, Ibrahim Nor Azowa. Synthesis, characterization, and antimicrobial properties of copper nanoparticles. *Int J Nanomed* 2013;4467–79.
- [30] Stevenson J, Barwinska-Sendra A, Tarrant E, Waldron KJ. Mechanism of action and applications of the antimicrobial properties of copper. *Microb. Pathog. Strateg. Combat. them Sci. Technol. Educ.* 2013;2:468–79.
- [31] Benli Hüseyin, Bahtiyari Muhammed Ibrahim, Aydınloğlu Ömer, Özen İlhan. Reuse of waste dye bathes for sustainable wool dyeing by depletion of metal salts and plant-based dyes. *J Clean Prod* 2024;450:141950.
- [32] Shah Vishal, Bhatt Manish, Stopka Pavel, Nerud František. Copper based Fenton's system for the decolorization of synthetic dyes and dye industry effluents. *Asian J Water Environ Pollut* 2005;2(1):61–4.
- [33] Rezaie, Ali Bashiri, Montazer Majid, Mahmoudi Rad Mahnaz. Scalable, eco-friendly and simple strategy for nano-functionalization of textiles using immobilized copper-based nanoparticles. *Clean Technol Environ Policy* 2018;20: 2119–33.
- [34] Ghosh Sougata, et al. Antidiabetic and antioxidant properties of copper nanoparticles synthesized by medicinal plant *Dioscorea bulbifera*. *J Nanomed Nanotechnol* 2015;S6:1.
- [35] Milne Lesley, Nicotera Pierluigi, Orrenius Sten, Burkitt Mark J. Effects of glutathione and chelating agents on copper-mediated DNA oxidation: pro-oxidant and antioxidant properties of glutathione. *Arch Biochem Biophys* 1993;304(1): 102–9.
- [36] Mozdzan Monika, Szemraj Janusz, Rysz Jacek, Nowak Dariusz. Antioxidant properties of carnosine re-evaluated with oxidizing systems involving iron and copper ions. *Basic Clin Pharmacol Toxicol* 2005;96(5):352–60.
- [37] Dutta Sabari, Ratnamala Bendre, Subhash Padhye, Ahmed Fakhara, Sarkar Fazlul. Synthesis, antioxidant properties and antiproliferative activities of tetrameric copper and copper-zinc metal complexes of catecholamine Schiff base ligand. *Synth. React. Inorganic, Met. Nano-Metal Chem.* 2005;35(1):3–10.
- [38] Kulkarni SS, V Gokhale A, Bodake UM, Pathade GR. Cotton dyeing with natural dye extracted from pomegranate (*punica granatum*) peel. *Univers. J. Environ. Res. Technol.* 2011;1(2).
- [39] Kechi Abera, Chavan RB, Moeckel Reinhart. Ethiopian dye plants as a source of natural dyes for cotton dyeing. *Univers. J. Environ. Res. Technol.* 2013;3(4).
- [40] Mirjalili Mohammad, Nazarpour Khosro, Karimi Loghman. Eco-friendly dyeing of wool using natural dye from weld as co-partner with synthetic dye. *J Clean Prod* 2011;19(9–10):1045–51.
- [41] Samanta Ashis Kumar. Application of natural dyes to cotton and jute textiles: science and technology and environmental issues. *Handb. Renew. Mater. Color. Finish.* 2018;16.
- [42] Ado A, Yahaya H, Kwali AA, Abdulkadir RS. Dyeing of textiles with eco-friendly natural dyes: a review. *Int. J. Environ. Monit. Prot.* 2014;1(5):76–81.
- [43] Bide Martin. Sustainable dyeing with synthetic dyes. Roadmap to Sustain. Text. Cloth. eco-friendly raw Mater. Technol. Process. Methods 2014:81–107.
- [44] Repon Reazuddin, Tauhidul Islam M, Mamun Abdullah Al, Rashid Muhammad Abdur. Comparative study on natural and reactive dye for cotton coloration. *J Appl Res Technol* 2018;16(3):160–9.
- [45] Lvov Yuri M, DeVilliers Melgardt M, Fakhru'llin Rawil F. The application of halloysite tubule nanoclay in drug delivery. *Expet Opin Drug Deliv* 2016;13(7): 977–86.
- [46] Liu Mingxian, Jia Zhixian, Jia Demin, Zhou Changren. Recent advance in research on halloysite nanotubes-polymer nanocomposite. *Prog Polym Sci* 2014;39(8): 1498–525.
- [47] Lazaratou Christina V, Panagiotaras Dionisios, Panagopoulos Georgios, Pospíšil Miroslav, Papoulis Dimitrios. Ca treated Palgorskite and Halloysite clay minerals for Ferrous Iron (Fe+2) removal from water systems. *Environ Technol Innov* 2020;19:100961. <https://doi.org/10.1016/j.eti.2020.100961>.
- [48] Van Ranst Eric, Kips Philip, Mbogoni Joseph, Mees Florias, Dumon Mathijs, Bruno Delvaux. Halloysite-smectite mixed-layered clay in fluvio-volcanic soils at the southern foot of Mount Kilimanjaro, Tanzania. *Geoderma* 2020;375(May): 114527. <https://doi.org/10.1016/j.geoderma.2020.114527>.
- [49] Zhao Ningning, Liu Yulin, Zhao Xiaomeng, Song Hongzan. Liquid crystal self-assembly of halloysite nanotubes in ionic liquids: a novel soft nanocomposite ionogel electrolyte with high anisotropic ionic conductivity and thermal stability. *Nanoscale* 2016;8(3):1545–54.
- [50] Lazzara Giuseppe, et al. An assembly of organic-inorganic composites using halloysite clay nanotubes. *Curr Opin Colloid Interface Sci* 2018;35:42–50.
- [51] Yendluri Raghuvara, Otto Daniel P, De Villiers Melgardt M, Vinokurov Vladimir, Lvov Yuri M. Application of halloyite clay nanotubes as a pharmaceutical excipient. *Int J Pharm* 2017;521(1–2):267–73.
- [52] Yuan Peng, Tan Daoyong, Annabi-Bergaya Faiza. Properties and applications of halloysite nanotubes: recent research advances and future prospects. *Appl Clay Sci* 2015;112:75–93.
- [53] Pasbakhsh Pooria, Jock Churchman G, Keeling John L. Characterisation of properties of various halloysites relevant to their use as nanotubes and microfibre fillers. *Appl Clay Sci* 2013;74:47–57.
- [54] Makaremi Maziyar, et al. Effect of morphology and size of halloysite nanotubes on functional pectin bionanocomposites for food packaging applications. *ACS Appl Mater Interfaces* 2017;9(20):17476–88.
- [55] Cavallaro Giuseppe, Chiappisi Leonardo, Pasbakhsh Pooria, Gradzielski Michael, Lazzara Giuseppe. A structural comparison of halloysite nanotubes of different origin by Small-Angle Neutron Scattering (SANS) and Electric Birefringence. *Appl Clay Sci* 2018;160:71–80.
- [56] Agafonov AV, Kudryakova NO, Ramenskaya LM, Grishina EP. The confinement and anion type effect on the physicochemical properties of ionic liquid/halloysite nanoclay ionogels. *Arab J Chem* 2020;13(12):9090–104. <https://doi.org/10.1016/j.arabjch.2020.10.033>.
- [57] Blagojević Bojana, Četojević-Simin Dragana, Parisi Filippo, Lazzara Giuseppe, Popović Boris M. Halloysite nanotubes as a carrier of cornelian cherry (*Cornus mas L.*) bioactives. *Lwt* 2020;134(June). <https://doi.org/10.1016/j.lwt.2020.110247>.
- [58] Zhang Baifa, et al. Effect of curing conditions on the microstructure and mechanical performance of geopolymers derived from nanosized tubular halloysite. *Construct Build Mater* 2020;121186. <https://doi.org/10.1016/j.conbuildmat.2020.121186>.
- [59] Luo Peng, Zhao Yafei, Zhang Bing, Liu Jindun, Yang Yong, Liu Junfang. Study on the adsorption of Neutral Red from aqueous solution onto halloysite nanotubes. *Water Res* 2010;44(5):1489–97.
- [60] Liu Wei, et al. Mixed hemimicelle solid-phase extraction based on magnetic halloysite nanotubes and ionic liquids for the determination and extraction of azo dyes in environmental water samples. *J Chromatogr. A* 2018;1551:10–20.
- [61] Zhao Mingfei, Peng Liu. Adsorption behavior of methylene blue on halloysite nanotubes. *Microporous Mesoporous Mater* 2008;112(1–3):419–24.
- [62] Luo Peng, Zhang Bing, Zhao Yafei, Zhang Jinhua, Zhang Haoqin, Liu Jindun. Removal of methylene blue from aqueous solutions by adsorption onto chemically activated halloysite nanotubes. *Kor J Chem Eng* 2011;28(3):800–7.
- [63] Liu Yi, Zheng Yian, Wang Aiqin. Response surface methodology for optimizing adsorption process parameters for methylene blue removal by a hydrogel composite. *Adsorpt Sci Technol* 2010;28(10):913–22.
- [64] Liu Lin, Wan Yazhen, Xie Yinde, Zhai Rui, Zhang Bing, Liu Jindun. The removal of dye from aqueous solution using alginate-halloysite nanotube beads. *Chem Eng J* 2012;187:210–6.
- [65] Peng Qi, Liu Mingxian, Zheng Jianwen, Zhou Changren. Adsorption of dyes in aqueous solutions by chitosan-halloysite nanotubes composite hydrogel beads. *Microporous Mesoporous Mater* 2015;201:190–201.

- [66] Jiang Ling, et al. Surface modifications of halloysite nanotubes with superparamagnetic Fe<sub>3</sub>O<sub>4</sub> nanoparticles and carbonaceous layers for efficient adsorption of dyes in water treatment. *Chem Res Chin Univ* 2014;30(6):971–7.
- [67] Nguyen Thi Kim Lien, Cao Xuan Thang, Park Chan, Lim Kwon Taek. Preparation, characterization and application of magnetic halloysite nanotubes for dye removal. *Mol Cryst Liq Cryst* 2017;644(1):153–9.
- [68] Wan Xinyi, Zhan Yingqing, Long Zhihang, Zeng Guangyong, He Yi. Core@double-shell structured magnetic halloysite nanotube nano-hybrid as efficient recyclable adsorbent for methylene blue removal. *Chem Eng J* 2017;330:491–504.
- [69] Farrokhi-Rad Morteza, Mohammadalipour Mehrdad, Shahrabi Taghi. Electrophoretically deposited halloysite nanotubes coating as the adsorbent for the removal of methylene blue from aqueous solution. *J Eur Ceram Soc* 2018;38(10):3650–9.
- [70] Liu Ruichao, Fu Keming, Zhang Bing, Mei Dandan, Zhang Haoqin, Liu Jindun. Removal of methyl orange by modified halloysite nanotubes. *J Dispersion Sci Technol* 2012;33(5):711–8.
- [71] Chen Hao, Zhao Jie, Wu Junyong, Yan Hua. Selective desorption characteristics of halloysite nanotubes for anionic azo dyes. *RSC Adv* 2014;4(30):15389–93.
- [72] Chen Hao, et al. Trapping characteristic of halloysite lumen for methyl orange. *Appl Surf Sci* 2015;347:769–76.
- [73] Ferrarini F, Bonetto LR, Crespo Janaina S, Giovanela M. Removal of Congo red dye from aqueous solutions using a halloysite-magnetite-based composite. *Water Sci Technol* 2016;73(9):2132–42.
- [74] Bessaha Fatiha, Mahrez Nouria, Bendenia Souhila, Kasmî Fatima, Marouf-Khelifa Kheira, Khelifa Amine. Characterization and spectroscopic study of a heat-treated and acid-leached halloysite used in Congo red adsorption. *Int. J. Intell. Eng. Syst.* 2017;10(3):272–9.
- [75] Fard F Shahamati, Akbari Somaye, Pajootan Elmira, Arami Mokhtar. Enhanced acidic dye adsorption onto the dendrimer-based modified halloysite nanotubes. *Desalination Water Treat* 2016;57(54):26222–39.
- [76] Zango Zakariyya Uba, Abu Bakar Noor Hana Hanif, Tan Wei Leng, Bakar Mohamad Abu. Enhanced removal efficiency of methyl red via the modification of halloysite nanotubes by copper oxide. *J Dispersion Sci Technol* 2018;39(1):148–54.
- [77] Cavallaro G, Gianguzza A, Lazzara G, Milioto S, Piazzese D. Alginate gel beads filled with halloysite nanotubes. *Appl Clay Sci* 2013;72:132–7.
- [78] Kiani Gholamreza, Dostali Mohammad, Ali Rostami, Khataee Ali R. Adsorption studies on the removal of Malachite Green from aqueous solutions onto halloysite nanotubes. *Appl Clay Sci* 2011;54(1):34–9.
- [79] Bessaha Fatiha, Marouf-Khelifa Kheira, Batonneau-Gener Isabelle, Khelifa Amine. Characterization and application of heat-treated and acid-leached halloysites in the removal of malachite green: adsorption, desorption, and regeneration studies. *Desalination Water Treat* 2016;57(31):14609–21.
- [80] Duan Jingmin, Liu Ruichao, Chen Tong, Zhang Bing, Liu Jindun. Halloysite nanotube-Fe<sub>3</sub>O<sub>4</sub> composite for removal of methyl violet from aqueous solutions. *Desalination* 2012;293:46–52.
- [81] Bonetto LR, Ferrarini F, De Marco C, Crespo JS, Guégan Régis, Giovanela M. Removal of methyl violet 2B dye from aqueous solution using a magnetic composite as an adsorbent. *J Water Process Eng* 2015;6:11–20.
- [82] Tao Di, Higaki Yujii, Ma Wei, Takahara Atsushi. Halloysite nanotube/polyelectrolyte hybrids as adsorbents for the quick removal of dyes from aqueous solution. *Chem Lett* 2015;44(11):1572–4.
- [83] Desai Sanjay, Pandey Astha, Dahiya MS. Application of hallosysite nanotubes in removal of auramine Y and auramine O dyes. *Int. J. PharmTech. Res.* 2017;10:62–76.
- [84] Khatri Nitasha, Tyagi Sanjiv, Rawtani Deepak. Removal of basic dyes auramine yellow and auramine O by halloysite nanotubes. *Int J Environ Waste Manag* 2016;17(1):44–59.
- [85] Mudhoo Ackmez, Kumar Gautam Ravindra, Ncibi Mohamed Chaker, Zhao Feiping, Garg Vinod Kumar, Sillanpää Mika. Green synthesis, activation and functionalization of adsorbents for dye sequestration. *Environ Chem Lett* 2019;17(1):157–93.
- [86] Riahi-Madvaar Ramin, Ali Taher Mohammad, Hamid Fazelirad. Synthesis and characterization of magnetic halloysite-iron oxide nanocomposite and its application for naphthol green B removal. *Appl Clay Sci* 2017;137:101–6.
- [87] Massaro Marina, Colletti Carmelo G, Lazzara Giuseppe, Guernelli Susanna, Noto Renato, RIELA Serena. Synthesis and characterization of halloysite-cyclodextrin nanosponges for enhanced dyes adsorption. *ACS Sustainable Chem Eng* 2017;5(4):3346–52.
- [88] Zhao Yafei, Abdullayev Elshad, Vasiliev Alexandre, Lvov Yuri. Halloysite nanotubule clay for efficient water purification. *J Colloid Interface Sci* 2013;406:121–9.
- [89] Al-Beladi Ahlam A, Kosa Samia A, Abdul Wahab Roswanira, Abdel Salam Mohamed. Removal of Orange G dye from water using halloysite nanoclay-supported ZnO nanoparticles. *Desalin. WATER Treat.* 2020;196:287–98.
- [90] Kananî-Jazî Mohammad Hassan, Akbari Somaye. Amino-dendritic and carboxyl functionalized halloysite nanotubes for highly efficient removal of cationic and anionic dyes: kinetic, isotherm, and thermodynamic studies. *J Environ Chem Eng* 2021;9(3):105214. <https://doi.org/10.1016/j.jece.2021.105214>.
- [91] Limousin G, Gaudet JP, Charlet L, Szentkneet Stephanie, Barthes V, Krimissa M. Sorption isotherms: a review on physical bases, modeling and measurement. *Appl. geochemistry* 2007;22(2):249–75.
- [92] Voudrias E, Fytianos K, Bozani E. Sorption-desorption isotherms of dyes from aqueous solutions and wastewaters with different sorbent materials. *Glob. Nest Int. J.* 2002;4(1):75–83.
- [93] Foo KY, Hameed BH. Porous structure and adsorptive properties of pineapple peel based activated carbons prepared via microwave assisted KOH and K<sub>2</sub>CO<sub>3</sub>. *Microporous Mesoporous Mater* 2012;148(1):191–5.
- [94] Daneshvar Ehsan, Vazirzadeh Arya, Ali Niazi, Kousha Masoud, Mu Naushad, Bhatnagar Amit. Desorption of methylene blue dye from brown macroalgae: effects of operating parameters, isotherm study and kinetic modeling. *J Clean Prod* 2017;152:443–53.
- [95] Redlich OJDL, Peterson DL. A useful adsorption isotherm. *J Phys Chem* 1959;63(6):1024.
- [96] Momina Shahadat Mohammad, Suzylawati Isamil. Study of the adsorption/desorption of MB dye solution using bentonite adsorbent coating. *J Water Process Eng* 2020;34(July 2019). <https://doi.org/10.1016/j.jwpe.2020.101155>.
- [97] Karadag Recep. Establishing a new international standard for natural dyed textile goods [Natural Organic Dye Standard (NODS)]. *J Nat Fibers* 2023;20(1):2162187.
- [98] Choudhury Asim Kumar Roy. Eco-friendly dyes and dyeing. *Adv. Mater. Technol. Environ.* 2018;2:145–76.
- [99] Guerra Eugenia, Llompert Maria, Garcia-Jares Carmen. Analysis of dyes in cosmetics: challenges and recent developments. *Cosmetics* 2018;5(3):47.
- [100] Zhang Chengjiang, Li Gongke, Zhang Zhuomin. A hydrazone covalent organic polymer based micro-solid phase extraction for online analysis of trace Sudan dyes in food samples. *J Chromatogr. A* 2015;1419:1–9.
- [101] Pars,Abdulkadir; "Influence OF BIO-mordant treatment on dyeing properties of wool fabric dyed with natural dye extract obtained from madder plant (rubia tinctorum L.)," in II. International edirne red symposium, p. 131..
- [102] Standard Global Organic Textile. Global organic textile standard. *Recuper. el.* 2008;27.
- [103] Maharjan Surendra, Liao Kang Shyang, Wang Alexander J, Curran Seamus A. Highly effective hydrophobic solar reflective coating for building materials: increasing total solar reflectance via functionalized anatase immobilization in an organosiloxane matrix. *Construct Build Mater* 2020;243:118189. <https://doi.org/10.1016/j.conbuildmat.2020.118189>.
- [104] Liu Yi, et al. Separation and identification of microplastics in marine organisms by TGA-FTIR-GC/MS: a case study of mussels from coastal China. *Environ Pollut* 2020;115946. <https://doi.org/10.1016/j.envpol.2020.115946>.
- [105] Umar Muneer, Ofem Michael Ikpi, Anwar Auwal Sani, Garba Salisu Abubakar. Thermogravimetric analysis (TGA) of PA6/G and PA6/GNP composites using two processing streams. *J. King Saud Univ. - Eng. Sci.*no. xxxx 2020. <https://doi.org/10.1016/j.jksues.2020.09.003>.
- [106] Corazzari Ingrid, Turci Francesco, Nisticò Roberto. TGA coupled with FTIR gas analysis to quantify the vinyl alcohol unit content in ethylene-vinyl alcohol copolymer. *Mater Lett* 2021;284:129030. <https://doi.org/10.1016/j.matlet.2020.129030>.
- [107] Shen Jianyi, Tu Mai, Chen Hu. Structural and varying surface acid/base properties of hydrothermal-derived MgAlO oxides calcined at varying temperatures. *J Solid State Chem* 1998;137(2):295–301. <https://doi.org/10.1006/jssc.1997.7739>.
- [108] Liu Yijun, Lotero Edgar, Goodwin James G, Mo Xunhua. Transesterification of poultry fat with methanol using Mg-Al hydroxalcite derived catalysts. *Appl Catal Gen* 2007;331(1):138–48. <https://doi.org/10.1016/j.apcata.2007.07.038>.
- [109] Grum F, Witzel RF, Stensby P. Evaluation of whiteness. *JOSA* 1974;64(2):210–5.
- [110] ASTM. Standard tables for reference solar spectral irradiances : direct normal and. *Astm* 2013;3(Reapproved):1–21. <https://doi.org/10.1520/G0173-03R20.2>.
- [111] Bordepong Sunaree, Bhongsuwan Darunee, Punggrassami Thongchai, Bhongsuwan Tripob. Characterization of hallosysite from thung yai district, nakhon si thammarat province, in southern Thailand. *Songklanakarín J Sci Technol* 2011;33(5).
- [112] Zatta Leandro, da Costa Gardolinski José Eduardo Ferreira, Wypych Fernando. Raw halloysite as reusable heterogeneous catalyst for esterification of lauric acid. *Appl Clay Sci* 2011;51(1–2):165–9.
- [113] Mehraban Z, Farzaneh F, Shafiekhani A. Synthesis and characterization of a new organic-inorganic hybrid NiO-chlorophyll-a as optical material. *Opt Mater* 2007;29(8):927–31.
- [114] Zhu Han, Du MingLiang, Zou MeiLing, Xu CongSheng, Fu YaQin. Green synthesis of Au nanoparticles immobilized on halloysite nanotubes for surface-enhanced Raman scattering substrates. *Dalton Trans* 2012;41(34):10465–71.
- [115] Yuan Peng, et al. Functionalization of halloysite clay nanotubes by grafting with  $\gamma$ -aminopropyltriethoxysilane. *J Phys Chem C* 2008;112(40):15742–51.
- [116] Cheng Hongfei, Frost Ray L, Yang Jing, Liu Qinfu, He Junkai. Infrared and infrared emission spectroscopic study of typical Chinese kaolinite and halloysite. *Spectrochim Acta Part A Mol Biomol Spectrosc* 2010;77(5):1014–20.
- [117] Joussein Emmanuel, Petit Sabine, Bruno Delvaux. Behavior of halloysite clay under formamide treatment. *Appl Clay Sci* 2007;35(1–2):17–24.
- [118] Mellouk Senia, et al. Intercalation of halloysite from Djebel Debagh (Algeria) and adsorption of copper ions. *Appl Clay Sci* 2009;44(3–4):230–6.
- [119] Szczepanik Beata, et al. The effect of chemical modification on the physico-chemical characteristics of halloysite: FTIR, XRF, and XRD studies. *J Mol Struct* 2015;1084:16–22.
- [120] Frost Ray L, Kristof Janos, Schmidt Jolene M, Theo Klopogge J. Raman spectroscopy of potassium acetate-intercalated kaolinites at liquid nitrogen temperature. *Spectrochim Acta Part A Mol Biomol Spectrosc* 2001;57(3):603–9.
- [121] Abidi Nouredine, Hequet Eric. Cotton fabric graft copolymerization using microwave plasma. I. Universal attenuated total reflectance-FTIR study. *J Appl Polym Sci* 2004;93(1):145–54.
- [122] Safapour Siyamak, Jameel Rather Luqman, Moradnejad Javad, Mir Shazia Shaheen. Functional and colorful wool textiles through ecological dyeing with lemon balm bio-dyes and mordants. *Fibers Polym* 2023;24(12):4357–70.

- [123] Safapour Siyamak, Toprak-Cavdur Tuba, Jameel Rather Luqman, Assiri Mohammed A, Shahid Mohammad. Enhancing the sustainability and hygiene in the dyeing of wool yarns with *Prangos ferulacea* Aerial Parts extract in conjunction with metal–biomordant combinations. *Fibers Polym* 2024;1–15.
- [124] Seif Manal A, Muna MHLJI. Evaluating the effect of seams on colour fastness properties of textile fabrics. *Int J Text Fash Technol (IJTFT)* 2016;6:1–14.
- [125] Saeed Ayesha, Hassan Komal, Sadaf Sadaf Shama. A review on colour fastness of natural dyed textiles. *Pakistan J. Sci. Ind. Res. Ser. A Phys. Sci.* 2023;66(2): 201–12.
- [126] Kitaguchi Saori, Kuramoto Kanya, Moridera Hitomi, Sato Tetsuya. Evaluation of instrumental methods for assessing colour fastness. *J Fiber Bioeng Inf* 2012;5(4): 399–409.
- [127] Rodiah MH, Noor Hafizah S, Noor Asiah H, Nurhafizah I, Norakma MN, Norazlina I. Extraction of natural dye from the mesocarp and exocarp of *Cocos nucifera*, textile dyeing, and colour fastness properties. *Mater Today Proc* 2022; 48:790–5.